Elasto/Visco-Plastic Deformation of Multi-Layered Shells of Revolution*

Shigeo TAKEZONO**, Kohji MIGITA***
and Akihisa HIRAKAWA****

This paper is concerned with an analytical formulation and a numerical solution of the elasto/visco-plastic problems of multi-layered shells of revolution under asymmetrical loads with application to a cylindrical shell. The analytical formulation is developed by extending Sanders' theory on elastic shells. It is assumed that the total strain rates are composed of an elastic part and a part due to visco-plasticity. The elastic strains are proportional to the stresses by Hooke's law. The visco-plastic strain rates are related to the stresses by Perzyna's equation. As a numerical example, the elasto/visco-plastic deformation of a two-layered cylindrical shell composed of a titanium and a mild steel layer subjected to locally distributed loads is analyzed. Numerical computations are carried out for three cases of the ratio of the thickness of the titanium layer to the shell thickness. It is found from the computations that stress distributions and deformation vary significantly depending on the thickness ratio.

Key Words: Structural Analysis, Multi - Layered Shells of Revolution, Elasto/ Visco- Plastic Deformation, Asymmetrical Loads, FDM

1. Introduction

Many investigations[(1)~(12)] of the elasto/visco-plastic deformation of shells of revolution have been conducted. These investigations, however, have been mostly concerned with the case of single-layered shells, and few studies on multi-layered shells have been reported in spite of their importance in engineering.

In this paper, the authors study the elasto/visco-plastic deformation of the multi-layered shells of revolution under general asymmetrical loads. The equations of equilibrium and the relations between strain and displacement are derived from Sanders' theory for thin shells[(13)]. As the constitutive relation, Hooke's law is used in the linear elastic range, and the elasto/visco-plastic equations by Perzyna[(14)] are employed in the plastic range.

In the case of the multi-layered shells, the relations between the generalized stresses and strains are different from those of single-layered shells, and therefore the basic differential equations derived are also different.

The basic differential equations for incremental values are numerically solved by a finite difference method and the solutions are obtained by summation of the incremental values.

As a numerical example, the elasto/visco-plastic deformation of a simply supported two-layered cylindrical shell composed of mild steel and titanium subjected to locally distributed loads is analyzed. Numerical computations have been carried out for three cases of the ratio of thickness of the titanium layer to shell thickness.

* Received 22nd March, 1988. Paper No. 87-0021 A
** Department of Energy Engineering, Toyohashi University of Technology, Tempaku-cho, Toyohashi, 440, Japan
*** Mitsubishi Heavy Industry Co., Ltd., Hohnoura-cho, Nagasaki, 850, Japan
**** Nohgata Tateishi Electric Co., Ltd., Kamisakai-tobikuma, Nohgata, 822, Japan

2. Analytical Formulations

2.1 Fundamental equations

If the middle surface of axisymmetrical shells is given by $r=r(s)$, where r is the distance from the axis and s is the meridional distance measured from a boundary along the middle surface, as shown in Fig. 1, the relations among the non-dimensional curvatures $\omega_\xi(=a/R_s)$, $\omega_\theta(=a/R_\theta)$ and the non-dimensional radius $\rho(=r/a)$ become:

$$\left.\begin{aligned}&\omega_\xi=-(\gamma'+\gamma^2)\omega_\theta,\ \omega_\theta=\sqrt{1-(\rho')^2}/\rho\\&\omega_\theta'=\gamma(\omega_\xi-\omega_\theta),\ \rho''/\rho=-\omega_\xi\omega_\theta\\&\gamma=\rho'/\rho,\ \xi=s/a,\ (\quad)'=d(\quad)/d\xi\end{aligned}\right\}\tag{1}$$

where a is the reference length. An arbitrary point of the shell can be expressed by the orthogonal coordinate system (ξ, θ, ζ).

Eliminating the transverse shear forces Q_ξ and Q_θ in the equilibrium equations in Sanders' theory [13] and writing in the rate forms, the following equations are obtained:

$$\left.\begin{aligned}&a\left[\frac{\partial}{\partial\xi}(\rho\dot N_\xi)+\frac{\partial\dot{\bar N}_{\xi\theta}}{\partial\theta}-\rho'\dot N_\theta\right]\\&\quad+\omega_\xi\left[\frac{\partial}{\partial\xi}(\rho\dot M_\xi)+\frac{\partial\dot{\bar M}_{\xi\theta}}{\partial\theta}-\rho'\dot M_\theta\right]\\&\quad+\frac{1}{2}(\omega_\xi-\omega_\theta)\frac{\partial\dot{\bar M}_{\xi\theta}}{\partial\theta}+a^2\rho\dot P_\xi=0\\&a\left[\frac{\partial\dot N_\theta}{\partial\theta}+\frac{\partial}{\partial\xi}(\rho\dot{\bar N}_{\xi\theta})+\rho'\dot{\bar N}_{\xi\theta}\right]\\&\quad+\omega_\theta\left[\frac{\partial\dot M_\theta}{\partial\theta}+\frac{\partial}{\partial\xi}(\rho\dot{\bar M}_{\xi\theta})+\rho'\dot{\bar M}_{\xi\theta}\right]\\&\quad+\frac{\rho}{2}\frac{\partial}{\partial\xi}[(\omega_\theta-\omega_\xi)\dot{\bar M}_{\xi\theta}]+a^2\rho\dot P_\theta=0\\&\frac{\partial}{\partial\xi}\left[\frac{\partial}{\partial\xi}(\rho\dot M_\xi)+\frac{\partial\dot{\bar M}_{\xi\theta}}{\partial\theta}-\rho'\dot M_\theta\right]\\&\quad+\frac{1}{\rho}\frac{\partial}{\partial\theta}\left[\frac{\partial\dot M_\theta}{\partial\theta}+\frac{\partial}{\partial\xi}(\rho\dot{\bar M}_{\xi\theta})+\rho'\dot{\bar M}_{\xi\theta}\right]\\&\quad-a\rho(\omega_\xi\dot N_\xi+\omega_\theta\dot N_\theta)+a^2\rho\dot P_\zeta=0\end{aligned}\right\}\tag{2}$$

where:

$$\left.\begin{aligned}&\dot{\bar N}_{\xi\theta}=(\dot N_{\xi\theta}+\dot N_{\theta\xi})/2\\&\qquad+[(1/R_\theta)-(1/R_s)](\dot M_{\xi\theta}-\dot M_{\theta\xi})/4\\&\dot{\bar M}_{\xi\theta}=(\dot M_{\xi\theta}+\dot M_{\theta\xi})/2\end{aligned}\right\}\tag{3}$$

and the notations are shown in Fig. 2.

$\hat N_{\xi\theta}$ and $\hat Q_\xi$ in Fig. 1 are effective membrane and transverse shear forces per unit length, respectively, defined as follows:

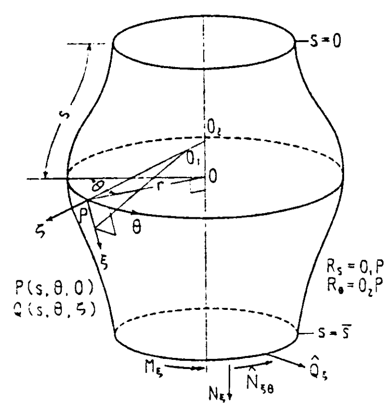

Fig. 1 Geometry and coordinates

$$\left.\begin{aligned}&\dot{\hat N}_{\xi\theta}=\dot{\bar N}_{\xi\theta}+\frac{1}{2}\left(\frac{3}{R_\theta}-\frac{1}{R_s}\right)\dot{\bar M}_{\xi\theta}\\&\dot{\hat Q}_\xi=\frac{1}{a\rho}\left[\frac{\partial}{\partial\xi}(\rho\dot M_\xi)+2\frac{\partial\dot{\bar M}_{\xi\theta}}{\partial\theta}-\rho'\dot M_\theta\right]\end{aligned}\right\}\tag{4}$$

The strain rates of the middle surface are given by:

$$\left.\begin{aligned}&\dot\varepsilon_{\xi m}=\frac{1}{a}\left[\frac{\partial\dot U_\xi}{\partial\xi}+\omega_\xi\dot U_\zeta\right]\\&\dot\varepsilon_{\theta m}=\frac{1}{a}\left[\frac{1}{\rho}\frac{\partial\dot U_\theta}{\partial\theta}+\gamma\dot U_\xi+\omega_\theta\dot U_\zeta\right]\\&\dot\varepsilon_{\xi\theta m}=\frac{1}{2a}\left[\frac{1}{\rho}\frac{\partial\dot U_\xi}{\partial\theta}+\frac{\partial\dot U_\theta}{\partial\xi}-\gamma\dot U_\theta\right]\end{aligned}\right\}\tag{5}$$

where $\dot\varepsilon_{\xi\theta m}$ is half the usual engineering shear strain rate. The bending distortion rates are as follows:

$$\left.\begin{aligned}&\dot\chi_\xi=\frac{1}{a}\frac{\partial\dot\Phi_\xi}{\partial\xi},\ \dot\chi_\theta=\frac{1}{a}\left(\frac{1}{\rho}\frac{\partial\dot\Phi_\theta}{\partial\theta}+\gamma\dot\Phi_\xi\right)\\&\dot\chi_{\xi\theta}=\frac{1}{2a}\left[\frac{1}{\rho}\frac{\partial\dot\Phi_\xi}{\partial\theta}+\frac{\partial\dot\Phi_\theta}{\partial\xi}-\gamma\dot\Phi_\theta\right.\\&\qquad\left.+\frac{1}{2a}(\omega_\xi-\omega_\theta)\left(\frac{1}{\rho}\frac{\partial\dot U_\xi}{\partial\theta}-\frac{\partial\dot U_\theta}{\partial\xi}-\gamma\dot U_\theta\right)\right]\end{aligned}\right\}\tag{6}$$

where rotation rates $\dot\Phi_\xi$ and $\dot\Phi_\theta$ are:

$$\left.\begin{aligned}&\dot\Phi_\xi=\frac{1}{a}\left(-\frac{\partial\dot U_\zeta}{\partial\xi}+\omega_\xi\dot U_\xi\right)\\&\dot\Phi_\theta=\frac{1}{a}\left(-\frac{1}{\rho}\frac{\partial\dot U_\zeta}{\partial\theta}+\omega_\theta\dot U_\theta\right)\end{aligned}\right\}\tag{7}$$

Under the Kirchhoff-Love hypothesis and the neglect of terms of order ζ/R_s and ζ/R_θ relative to unity, the strain rates at the distance ζ from the middle surface are:

$$\{\dot\varepsilon\}=\{\dot\varepsilon_m\}+\zeta\{\dot\chi\}\tag{8}$$

where

$$\left.\begin{aligned}&\{\dot\varepsilon\}=\{\dot\varepsilon_\xi,\ \dot\varepsilon_\theta,\ \dot\varepsilon_{\xi\theta}\}^T,\ \{\dot\varepsilon_m\}=\{\dot\varepsilon_{\xi m},\ \dot\varepsilon_{\theta m},\ \dot\varepsilon_{\xi\theta m}\}^T\\&\{\dot\chi\}=\{\dot\chi_\xi,\ \dot\chi_\theta,\ \dot\chi_{\xi\theta}\}^T\end{aligned}\right\}\tag{9}$$

Now, we shall use the elasto/visco-plastic equa-

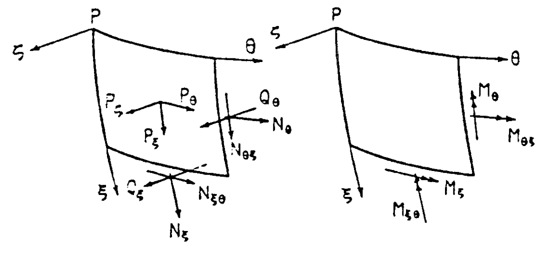

(a) Forces and loads (b) Moments

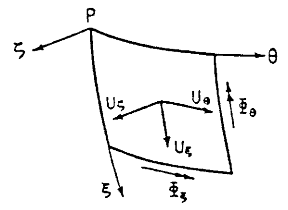

(c) Displacements and Rotations

Fig. 2 Notations

tions by Perzyna[14] for the constitutive relations

$$\dot{\varepsilon}_{ij}=\frac{1+\nu}{E}\dot{S}_{ij}+\frac{1-2\nu}{E}\dot{S}\delta_{ij}+\gamma_0\langle\Phi(F)\rangle S_{ij}J_2^{-1/2} \qquad (10)$$

where the dot denotes partial differentiation with respect to time; ε_{ij}, S, S_{ij} and J_2 are strain, mean stress, deviatoric stress and the second invariant, respectively; and E, ν and γ_0 are Young's modulus, Poisson's ratio and the viscosity constant of the material. The symbol $\langle\Phi(F)\rangle$ is defined as follows:

$$\left.\begin{aligned}\langle\Phi(F)\rangle&=0,\ F\leqq 0\\ &=\Phi(F),\ F>0\end{aligned}\right\} \qquad (11)$$

where function F is:

$$F=(\bar{\sigma}-\sigma^*)/\sigma^* \qquad (12)$$

and $F=0$ denotes the von Mises yield surface, $\bar{\sigma}$ is the equivalent stress $(=\sqrt{3J_2})$ and σ^* is the statical stress determined from the elasto-plastic stress-strain relation in a usual tension test.

In the plane stress state, as usually assumed in ordinary shell theories, the constitutive relation (10) may be expressed as follows:

$$\{\dot{\varepsilon}\}=[D]^{-1}\{\dot{\sigma}\}+\{\dot{\varepsilon}^{vp}\} \qquad (13)$$

where

$$\left.\begin{aligned}&\{\dot{\sigma}\}=\{\dot{\sigma}_\xi,\ \dot{\sigma}_\theta,\ \dot{\sigma}_{\xi\theta}\}^T,\ \{\dot{\varepsilon}^{vp}\}=\{\dot{\varepsilon}_\xi^{vp},\ \dot{\varepsilon}_\theta^{vp},\ \dot{\varepsilon}_{\xi\theta}^{vp}\}^T\\ &[D]=\frac{E}{1-\nu^2}\begin{bmatrix}1 & \nu & 0\\ \nu & 1 & 0\\ 0 & 0 & 1-\nu\end{bmatrix}\end{aligned}\right\} \qquad (14)$$

$$\left.\begin{aligned}&\{\dot{\varepsilon}^{vp}\}=\gamma_1\left\langle\Phi\left(\frac{\bar{\sigma}-\sigma^*}{\sigma^*}\right)\right\rangle\frac{1}{\bar{\sigma}}\begin{bmatrix}1 & -1/2 & 0\\ -1/2 & 1 & 0\\ 0 & 0 & 3/2\end{bmatrix}\{\sigma\}\\ &\gamma_1=(2/\sqrt{3})\gamma_0\end{aligned}\right. \qquad (15)$$

Substituting Eqs.(8) into Eqs.(13) and solving them for stress rates, the stress rates are given:

$$\{\dot{\sigma}\}=[D][\{\dot{\varepsilon}_m\}+\zeta\{\dot{\chi}\}]-\{\dot{\sigma}^{vp}\} \qquad (16)$$

where

$$\{\dot{\sigma}^{vp}\}=[D]\{\dot{\varepsilon}^{vp}\} \qquad (17)$$

From Eqs.(16), the rates of change of the resultant forces and the resultant moments for the multi-layered shell (Fig. 3) may be expressed by the following:

$$\left.\begin{aligned}\begin{Bmatrix}\dot{N}\\ \dot{M}\end{Bmatrix}&=\int_{-h/2}^{h/2}\begin{Bmatrix}\dot{\sigma}\\ \dot{\sigma}\zeta\end{Bmatrix}d\zeta=\sum_{i=1}^{n}\int_{\zeta_{i-1}}^{\zeta_i}\begin{Bmatrix}\dot{\sigma}\\ \dot{\sigma}\zeta\end{Bmatrix}d\zeta\\ &=\begin{bmatrix}\bar{A} & \bar{B}\\ \bar{B} & \bar{C}\end{bmatrix}\begin{Bmatrix}\dot{\varepsilon}_m\\ \dot{\chi}\end{Bmatrix}-\begin{Bmatrix}\dot{N}^{vp}\\ \dot{M}^{vp}\end{Bmatrix}\end{aligned}\right\} \qquad (18)$$

where

$$\left.\begin{aligned}&\{\dot{N}\}=\{\dot{N}_\xi,\ \dot{N}_\theta,\ \dot{\bar{N}}_{\xi\theta}\}^T,\ \{\dot{M}\}=\{\dot{M}_\xi,\ \dot{M}_\theta,\ \dot{\bar{M}}_{\xi\theta}\}^T\\ &\{\dot{N}^{vp}\}=\{\dot{N}_\xi^{vp},\ \dot{N}_\theta^{vp},\ \dot{\bar{N}}_{\xi\theta}^{vp}\}^T=\int_{-h/2}^{h/2}\{\dot{\sigma}^{vp}\}d\zeta\\ &\quad=\sum_{i=1}^{n}[D_i]\int_{\zeta_{i-1}}^{\zeta_i}\{\dot{\varepsilon}^{vp}\}d\zeta\\ &\{\dot{M}^{vp}\}=\{\dot{M}_\xi^{vp},\ \dot{M}_\theta^{vp},\ \dot{\bar{M}}_{\xi\theta}^{vp}\}^T=\int_{-h/2}^{h/2}\{\dot{\sigma}^{vp}\}\zeta d\zeta\\ &\quad=\sum_{i=1}^{n}[D_i]\int_{\zeta_{i-1}}^{\zeta_i}\{\dot{\varepsilon}^{vp}\}\zeta d\zeta\\ &[D_i]=\frac{E_i}{1-\nu_i^2}\begin{bmatrix}1 & \nu_i & 0\\ \nu_i & 1 & 0\\ 0 & 0 & 1-\nu_i\end{bmatrix}\end{aligned}\right\} \qquad (19)$$

and

$$\left.\begin{aligned}\bar{A}&=\int_{-h/2}^{h/2}[D]d\zeta=\sum_{i=1}^{n}[D_i]\int_{\zeta_{i-1}}^{\zeta_i}d\zeta\\ &=\sum_{i=1}^{n}[D_i](\zeta_i-\zeta_{i-1})\\ \bar{B}&=\int_{-h/2}^{h/2}[D]\zeta d\zeta=\sum_{i=1}^{n}[D_i]\int_{\zeta_{i-1}}^{\zeta_i}\zeta d\zeta\\ &=\frac{1}{2}\sum_{i=1}^{n}[D_i](\zeta_i^2-\zeta_{i-1}^2)\\ \bar{C}&=\int_{-h/2}^{h/2}[D]\zeta^2 d\zeta=\sum_{i=1}^{n}[D_i]\int_{\zeta_{i-1}}^{\zeta_i}\zeta^2 d\zeta\\ &=\frac{1}{3}\sum_{i=1}^{n}[D_i](\zeta_i^3-\zeta_{i-1}^3)\end{aligned}\right\} \qquad (20)$$

In Eqs.(18)～(20), the subscript i refers to the ith layer.

A complete set of field equations for 32 independent variables: $\dot{N}_\xi$, $\dot{N}_\theta$, $\dot{\bar{N}}_{\xi\theta}$, $\dot{M}_\xi$, $\dot{M}_\theta$, $\dot{\bar{M}}_{\xi\theta}$, $\dot{U}_\xi$, $\dot{U}_\theta$, $\dot{U}_\zeta$, $\dot{\varepsilon}_{\xi m}$, $\dot{\varepsilon}_{\theta m}$, $\dot{\varepsilon}_{\xi\theta m}$, $\dot{\chi}_\xi$, $\dot{\chi}_\theta$, $\dot{\chi}_{\xi\theta}$, $\dot{\Phi}_\xi$, $\dot{\Phi}_\theta$, $\dot{\sigma}_\xi$, $\dot{\sigma}_\theta$, $\dot{\sigma}_{\xi\theta}$, $\dot{\sigma}_\xi^{vp}$, $\dot{\sigma}_\theta^{vp}$, $\dot{\sigma}_{\xi\theta}^{vp}$, $\dot{\varepsilon}_\xi^{vp}$, $\dot{\varepsilon}_\theta^{vp}$, $\dot{\varepsilon}_{\xi\theta}^{vp}$, $\dot{N}_\xi^{vp}$, $\dot{N}_\theta^{vp}$, $\dot{\bar{N}}_{\xi\theta}^{vp}$, $\dot{M}_\xi^{vp}$, $\dot{M}_\theta^{vp}$, $\dot{\bar{M}}_{\xi\theta}^{vp}$ is now given by 32 equations: (2), (5)～(7), (15)～(19).

2.2 Non-dimensional equations

It is assumed that the distributed loads and the 29 independent variables, except $\{\dot{\varepsilon}^{vp}\}$, can be expanded into Fourier series as follows:

$$\left.\begin{aligned}&\{\dot{P}_\xi,\ \dot{P}_\zeta,\ \dot{P}_\theta\}=(\sigma_0 h_0/a)\sum_{n=0}^{\infty}\{\dot{p}_\xi^{(n)},\ \dot{p}_\zeta^{(n)},\ \dot{p}_\theta^{(n)}\}\quad[A_n]\\ &\{\dot{N}_\xi,\ \dot{N}_\theta,\ \dot{\bar{N}}_{\xi\theta}\}=\sigma_0 h_0\sum_{n=0}^{\infty}\{\dot{n}_\xi^{(n)},\ \dot{n}_\theta^{(n)},\ \dot{n}_{\xi\theta}^{(n)}\}\quad[A_n]\\ &\{\dot{M}_\xi,\ \dot{M}_\theta,\ \dot{\bar{M}}_{\xi\theta}\}=(\sigma_0 h_0^3/a)\sum_{n=0}^{\infty}\{\dot{m}_\xi^{(n)},\ \dot{m}_\theta^{(n)},\ \dot{m}_{\xi\theta}^{(n)}\}\quad[A_n]\\ &\{\dot{U}_\xi,\ \dot{U}_\zeta,\ \dot{U}_\theta\}=(a\sigma_0/E_0)\sum_{n=0}^{\infty}\{\dot{u}_\xi^{(n)},\ \dot{u}_\zeta^{(n)},\ \dot{u}_\theta^{(n)}\}\quad[A_n]\\ &\{\dot{\varepsilon}_{\xi m},\ \dot{\varepsilon}_{\theta m},\ \dot{\varepsilon}_{\xi\theta m}\}\\ &\quad=(\sigma_0/E_0)\sum_{n=0}^{\infty}\{\dot{e}_{\xi m}^{(n)},\ \dot{e}_{\theta m}^{(n)},\ \dot{e}_{\xi\theta m}^{(n)}\}\quad[A_n]\end{aligned}\right.$$

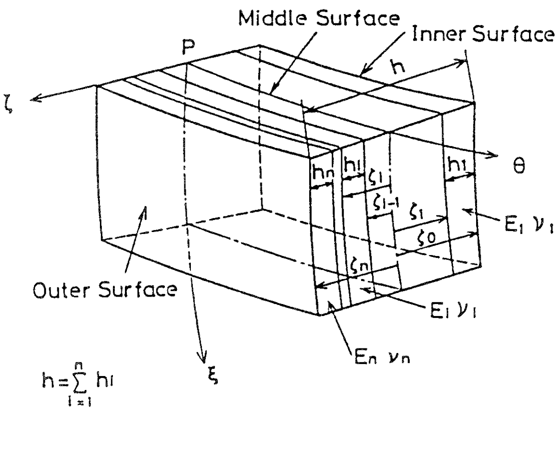

Fig. 3 Multi-layered shell element

$$\left.\begin{aligned}
&\{\dot\chi_\xi,\ \dot\chi_\theta,\ \dot\chi_{\xi\theta}\}=(\sigma_0/aE_0)\sum_{n=0}^{\infty}\{\dot k_\xi^{(n)},\ \dot k_\theta^{(n)},\ \dot k_{\xi\theta}^{(n)}\}\quad[A_n]\\
&\{\dot\Phi_\xi,\ \dot\Phi_\theta\}=(\sigma_0/E_0)\sum_{n=0}^{\infty}\{\dot\phi_\xi^{(n)}\cos n\theta,\ \dot\phi_\theta^{(n)}\sin n\theta\}\\
&\{\dot N_\xi^{vp},\ \dot N_\theta^{vp},\ \dot{\bar N}_{\xi\theta}^{vp}\}\\
&\quad=\sigma_0 h_0\sum_{n=0}^{\infty}\{\dot n_\xi^{vp(n)},\ \dot n_\theta^{vp(n)},\ \dot n_{\xi\theta}^{vp(n)}\}\quad[A_n]\\
&\{\dot M_\xi^{vp},\ \dot M_\theta^{vp},\ \dot{\bar M}_{\xi\theta}^{vp}\}\\
&\quad=(\sigma_0 h_0^3/a)\sum_{n=0}^{\infty}\{\dot m_\xi^{vp(n)},\ \dot m_\theta^{vp(n)},\ \dot m_{\xi\theta}^{vp(n)}\}\quad[A_n]\\
&\{\dot\sigma_\xi,\ \dot\sigma_\theta,\ \dot\sigma_{\xi\theta}\}=\sigma_0\sum_{n=0}^{\infty}\{\dot s_\xi^{(n)},\ \dot s_\theta^{(n)},\ \dot s_{\xi\theta}^{(n)}\}\quad[A_n]\\
&\{\dot\sigma_\xi^{vp},\ \dot\sigma_\theta^{vp},\ \dot\sigma_{\xi\theta}^{vp}\}\\
&\quad=\sigma_0\sum_{n=0}^{\infty}\{\dot s_\xi^{vp(n)},\ \dot s_\theta^{vp(n)},\ \dot s_{\xi\theta}^{vp(n)}\}\quad[A_n]
\end{aligned}\right\}\qquad(21)$$

where

$$[A_n]=[\cos n\theta,\ \cos n\theta,\ \sin n\theta],\quad\text{(diagonal matrix)},\qquad(22)$$

and σ_0, h_0 and E_0 are a reference stress, a reference thickness, and a reference Young's modulus, respectively.

It should be noted that the Fourier expansions (21) are not the most general that could exist. For full generality, these expansions should be augmented by the additional series,

$$\{\dot P_\xi,\ \dot P_\zeta,\ \dot P_\theta\}=(\sigma_0 h_0/a)\sum_{n=0}^{\infty}\{\dot{\bar p}_\xi^{(n)},\ \dot{\bar p}_\zeta^{(n)},\ \dot{\bar p}_\theta^{(n)}\}\quad[B_n]\qquad(23)$$

where $[B_n]=[\sin n\theta,\ \sin n\theta,\ \cos n\theta]$, (diagonal matrix).

Equations (21) are substituted into the above fundamental equations as follows:

The equilibrium Eq. (2) lead to

$$\left.\begin{aligned}
&\dot n_\xi'+\gamma(\dot n_\xi-\dot n_\theta)+(n/\rho)\dot n_{\xi\theta}+\lambda^2\{\omega_\xi\dot m_\xi'\\
&\quad+\gamma\omega_\xi(\dot m_\xi-\dot m_\theta)+(n/2\rho)(3\omega_\xi-\omega_\theta)\dot m_{\xi\theta}\}\\
&\quad+\dot p_\xi=0\\
&\dot n_{\xi\theta}'+2\gamma\dot n_{\xi\theta}-(n/\rho)\dot n_\theta+\lambda^2\{-(n/\rho)\omega_\theta\dot m_\theta\\
&\quad+(1/2)(3\omega_\theta-\omega_\xi)\dot m_{\xi\theta}'+(1/2)[\gamma(3\omega_\theta+\omega_\xi')\\
&\quad-\omega_\xi]\dot m_{\xi\theta}\}+\dot p_\theta=0\\
&\quad-\omega_\xi\dot n_\xi-\omega_\theta\dot n_\theta+\lambda^2\{\dot m_\xi''+2\gamma\dot m_\xi'-\omega_\xi\omega_\theta\dot m_\xi\\
&\quad+[\omega_\xi\omega_\theta-(n/\rho)^2]\dot m_\theta-\gamma\dot m_\theta'+(2n/\rho)\dot m_{\xi\theta}'\\
&\quad+(2\gamma n/\rho)\dot m_{\xi\theta}\}+\dot p_\zeta=0
\end{aligned}\right\}\qquad(24)$$

where the superscript (n) on Fourier coefficients is omitted for convenience.

The relations (5)～(7) become

$$\left.\begin{aligned}
&\dot e_{\xi m}=\dot u_\xi'+\omega_\xi\dot u_\zeta,\ \dot e_{\theta m}=(n/\rho)\dot u_\theta+\gamma\dot u_\xi+\omega_\theta\dot u_\zeta\\
&\dot e_{\xi\theta m}=(1/2)[\dot u_\theta'-\gamma\dot u_\theta-(n/\rho)\dot u_\xi]\\
&\dot k_\xi=\dot\phi_\xi',\ \dot k_\theta=(n/\rho)\dot\phi_\theta+\gamma\dot\phi_\xi\\
&\dot k_{\xi\theta}=(1/2)\{-(n/\rho)\dot\phi_\xi+\dot\phi_\theta'+\gamma\dot\phi_\theta\\
&\quad+(1/2)(\omega_\theta-\omega_\xi)[(n/\rho)\dot u_\xi+\dot u_\theta'+\gamma\dot u_\theta]\}\\
&\dot\phi_\xi=-\dot u_\zeta'+\omega_\xi\dot u_\xi,\ \dot\phi_\theta=(n/\rho)\dot u_\zeta+\omega_\theta\dot u_\theta
\end{aligned}\right\}\qquad(25)$$

and Eqs. (18) lead to

$$\left.\begin{aligned}
&\dot n_\xi=A_1\dot e_{\xi m}+A_2\dot e_{\theta m}+B_1\dot k_\xi+B_2\dot k_\theta-\dot n_\xi^{vp}\\
&\dot n_\theta=A_1\dot e_{\theta m}+A_2\dot e_{\xi m}+B_1\dot k_\theta+B_2\dot k_\xi-\dot n_\theta^{vp}\\
&\dot n_{\xi\theta}=A_3\dot e_{\xi\theta m}+B_3\dot k_{\xi\theta}-\dot n_{\xi\theta}^{vp}\\
&\dot m_\xi=(B_1/\lambda^2)\dot e_{\xi m}+(B_1/\lambda^2)\dot e_{\theta m}\\
&\quad+C_1\dot k_\xi+C_2\dot k_\theta-\dot m_\xi^{vp}\\
&\dot m_\theta=(B_1/\lambda^2)\dot e_{\theta m}+(B_2\lambda^2)\dot e_{\xi m}\\
&\quad+C_1\dot k_\theta+C_2k_\xi-\dot m_\theta^{vp}\\
&\dot m_{\xi\theta}=(B_3/\lambda^2)\dot e_{\xi\theta m}+C_3\dot k_{\xi\theta}-\dot m_{\xi\theta}^{vp}
\end{aligned}\right\}\qquad(26)$$

where

$$\left.\begin{aligned}
&\begin{bmatrix}A_1&A_2&0\\A_2&A_1&0\\0&0&A_3\end{bmatrix}=\frac{\bar A}{h_0E_0},\ \begin{bmatrix}B_1&B_2&0\\B_2&B_1&0\\0&0&B_3\end{bmatrix}=\frac{\bar B}{ah_0E_0}\\
&\begin{bmatrix}C_1&C_2&0\\C_2&C_1&0\\0&0&C_3\end{bmatrix}=\frac{\bar C}{h_0^3E_0},\ \lambda=h_0/a
\end{aligned}\right\}\qquad(27)$$

For each n, the set of field equations for the 17 Fourier coefficients $\dot n_\xi$, $\dot n_\theta$, $\dot n_{\xi\theta}$, $\dot m_\xi$, $\dot m_\theta$, $\dot m_{\xi\theta}$, $\dot u_\xi$, $\dot u_\theta$, $\dot u_\zeta$, $\dot\phi_\xi$, $\dot\phi_\theta$, $\dot e_{\xi m}$, $\dot e_{\theta m}$, $\dot e_{\xi\theta m}$, $\dot k_\xi$, $\dot k_\theta$, $\dot k_{\xi\theta}$ is now given by the 17 Eqs. (24)～(26).

By eliminating $\dot k_\xi$ from Eqs. $(26)_{1,4}$, Eqs. $(26)_{2,4}$ and Eqs. $(26)_{4,5}$, the following equations are obtained, respectively:

$$\left.\begin{aligned}
&\dot n_\xi=(B_1/C_1)\dot m_\xi+[A_1-(B_1^2/\lambda^2C_1)]\dot e_{\xi m}\\
&\quad+[A_2-(B_1B_2/\lambda^2C_1)]\dot e_{\theta m}+[B_2-(B_1C_2/C_1)]\dot k_\theta\\
&\quad-\dot n_\xi^{vp}+(B_1/C_1)\dot m_\xi^{vp}\\
&\dot n_\theta=(B_2/C_1)\dot m_\xi+[A_2-(B_1B_2/\lambda^2C_1)]\dot e_{\xi m}\\
&\quad+[A_1-(B_2^2/\lambda^2C_1)]\dot e_{\theta m}+[B_1-(B_2C_2/C_1)]\dot k_\theta\\
&\quad-\dot n_\theta^{vp}+(B_2C_1)\dot m_\xi^{vp}\\
&\dot m_\theta=(C_2/C_1)\dot m_\xi+(1/\lambda^2)[B_2-(B_1C_2/C_1)]\dot e_{\xi m}\\
&\quad+(1/\lambda^2)[B_1-(B_2C_2/C_1)]\dot e_{\theta m}\\
&\quad+[C_1-(C_2^2/C_1)]\dot k_\theta\\
&\quad-\dot m_\theta^{vp}+(C_2/C_1)\dot m_\xi^{vp}
\end{aligned}\right\}\qquad(28)$$

Substituting Eqs. $(26)_{3,6}$ and (28) into Eqs. (24) and using Eqs. (25) to eliminate the membrane strains and bending distortions gives three equations convenient for numerical computations, which have second-order derivatives of the variables u_ξ, u_θ, u_ζ and m_ξ. The fourth equation may be obtained from substitution of Eqs. (25) into Eq. $(26)_4$.

The resultant set of equations can be written as:

$$\left.\begin{aligned}
&a_1\dot u_\xi''+a_2\dot u_\xi'+a_3\dot u_\xi+a_4\dot u_\theta'+a_5\dot u_\theta+a_6\dot u_\zeta''\\
&\quad+a_7\dot u_\zeta'+a_8\dot u_\zeta+a_9\dot m_\xi'+a_{10}\dot m_\xi=c_1\\
&a_{11}\dot u_\xi'+a_{12}\dot u_\xi+a_{13}\dot u_\theta''+a_{14}\dot u_\theta'+a_{15}\dot u_\theta+a_{16}\dot u_\zeta''\\
&\quad+a_{17}\dot u_\zeta'+a_{18}\dot u_\zeta+a_{19}\dot m_\xi=c_2\\
&a_{20}\dot u_\xi''+a_{21}\dot u_\xi'+a_{22}\dot u_\xi+a_{23}\dot u_\theta''+a_{24}\dot u_\theta'+a_{25}\dot u_\theta\\
&\quad+a_{26}\dot u_\zeta''+a_{27}\dot u_\zeta'+a_{28}\dot u_\zeta+a_{29}\dot m_\xi''+a_{30}\dot m_\xi'\\
&\quad+a_{31}\dot m_\xi=c_3\\
&a_{32}\dot u_\xi'+a_{33}\dot u_\xi+a_{34}\dot u_\theta+a_{35}\dot u_\zeta''+a_{36}\dot u_\zeta'\\
&\quad+a_{37}\dot u_\zeta+a_{38}\dot m_\xi=c_4
\end{aligned}\right\}\qquad(29)$$

where a_1～a_{38} are constants which depend on shell form and materials, and c_1～c_4 are determined from the loads, and the membrane forces and moments due to visco-plasticity. These are given as follows:

$$a_1=A_1-B_1^2/(\lambda^2C_1),\ a_2=\gamma a_1$$

$$
\begin{aligned}
a_3 =& (\gamma\omega'_\xi - \omega_\xi^2\omega_\theta)B_2 - \gamma^2 A_1 - 2\gamma^2\omega_\xi B_1 \\
&+ (1/2)(n/\rho)^2(\omega_\theta - 3\omega_\xi)B_3 - \omega_\xi\omega_\theta A_2 \\
&- (1/2)(n/\rho)^2 A_3 - \lambda^2\gamma^2\omega_\xi^2 C_1 - (1/8)(n/\rho)^2\lambda^2(\omega_\theta \\
&- 3\omega_\xi)^2 C_3 + (\omega_\xi^2\omega_\theta - \gamma\omega'_\xi)B_1 C_2/C_1 \\
&+ \omega_\xi\omega_\theta B_1 B_1/(\lambda^2 C_1) + \gamma^2 B_2^2/(\lambda^2 C_1) \\
&+ 2\gamma^2\omega_\xi B_2 C_2/C_1 + \lambda^2\gamma^2\omega_\xi^2 C_2^2/C_1 \\
a_4 =& (n/\rho)A_2 + (n/\rho)\omega_\theta B_2 + (1/2)(n/\rho)A_3 \\
&+ (1/2)(n/\rho)(\omega_\theta + \omega_\xi)B_3 + (1/8)(n/\rho)\lambda^2(3\omega_\xi \\
&- \omega_\theta)(3\omega_\theta - \omega_\xi)C_3 - (n/\rho)B_1 B_2/(\lambda^2 C_1) \\
&- (n/\rho)\omega_\theta B_1 C_2/C_1 \\
a_5 =& -\gamma(n/\rho)A_1 - (\gamma/2)(n/\rho)A_3 - (\gamma/2)(n/\rho)(\omega_\xi \\
&+ \omega_\theta)B_3 + (\gamma/8)(n/\rho)\lambda^2(3\omega_\xi - \omega_\theta)(\omega_\xi - 3\omega_\theta)C_3 \\
&- (n/\rho)\gamma(\omega_\xi - \omega_\theta)B_1 C_2/C_1 + (\gamma/\lambda^2)(n/\rho)B_2^2/C_1 \\
&- \gamma(n/\rho)(\omega_\theta + \omega_\xi)(B_1 - B_2 C_2/C_1) \\
&+ (n\gamma/\rho)(\omega_\xi - \omega_\theta)B_2 \\
&- \lambda^2 r(n/\rho)\omega_\xi\omega_\theta(C_1 - C_2^2/C_1) \\
a_6 =& -\gamma(B_2 - B_1 C_2/C_1) \\
a_7 =& \omega_\xi A_1 + \omega_\theta A_2 + \{(n/\rho)^2 + \omega_\xi\omega_\theta\}B_2 + \gamma^2 B_1 \\
&+ (n/\rho)^2 B_3 + \lambda^2\gamma^2\omega_\xi C_1 + (\lambda^2/2)(n/\rho)^2(3\omega_\xi \\
&- \omega_\theta)C_3 - \omega_\xi B_1^2/(\lambda^2 C_1) \\
&- \omega_\theta B_1 B_2/(\lambda^2 C_1) - \{(n/\rho)^2 \\
&+ \omega_\xi\omega_\theta\}B_1 C_2/C_1 - \gamma^2 B_2 C_2/C_1 - \lambda^2\gamma^2\omega_\xi C_2^2/C_1 \\
a_8 =& (\omega'_\xi + \gamma\omega_\xi - \gamma\omega_\theta)A_1 - \gamma\{(n/\rho)^2 + \omega_\xi\omega_\theta\}B_1 \\
&- \gamma^2\gamma\omega_\xi(n/\rho)^2 C_1 - \gamma(n/\rho)^2 B_3 \\
&- (\gamma/2)(n/\rho)^2\lambda^2(3\omega_\xi - \omega_\theta)C_3 \\
&- (\omega'_\xi + \gamma\omega_\xi)B_1^2/(\lambda^2 C_1) + \gamma\omega_\theta B_2^2/(\lambda^2 C_1) \\
&+ \gamma\{(n/\rho)^2 + \omega_\xi\}B_1 C_2/C_1 \\
&+ \lambda^2\gamma\omega_\xi(n/\rho)^2 C_2^2/C_1 \\
&- \gamma\{\omega_\xi^2 + (n/\rho)^2\}B_2 + \gamma\{\omega_\xi\omega_\theta + (n/\rho)^2\}B_2 C_2/C_1 \\
a_9 =& B_1/C_1 + \lambda^2\omega_\xi \\
a_{10} =& (\gamma/C_1)\{B_1 - B_2 + \lambda^2\omega_\xi(C_1 - C_2)\} \qquad \text{etc.}
\end{aligned} \tag{30}
$$

$$
\left.
\begin{aligned}
c_1 =& -\dot{p}_\xi + \dot{n}_\xi^{vp\prime} + \gamma\dot{n}_\xi^{vp} - \gamma\dot{n}_\theta^{vp} + (n/\rho)\dot{n}_{\xi\theta}^{vp} \\
&- (B_1/C_1)\dot{m}_\xi^{vp\prime} + (\gamma/C_1)(B_2 - B_1 + \lambda^2\omega_\xi C_2)\dot{m}_\xi^{vp} \\
&- \lambda^2\gamma\omega_\xi\dot{m}_\theta^{vp} + (n\lambda^2/2\rho)(3\omega_\xi - \omega_\theta)\dot{m}_{\xi\theta}^{vp} \qquad \text{etc.}
\end{aligned}
\right\} \tag{31}
$$

If $i=1$, $\zeta_1=h/2$, $\zeta_0=-h/2$ are assumed in Eqs. (20), then $\bar{B}=0$, and Eqs. (29) ～ (31) coincide with the equations for single-layered shells previously derived by Takezono and Tao[5].

Once the solutions for $\dot{u}_\xi$, $\dot{u}_\theta$, $\dot{u}_\zeta$ and $\dot{m}_\xi$ have been calculated, the internal forces at any point in the shells can be found.

The stress rates (in the i th layer) can be expressed with the solution $\{\dot{z}\}$ of Eqs. (29) as follows:

$$\{\dot{s}_i\} = \{F_i\}\{\dot{z}\}' + \{H_i\}\{\dot{z}\} + \{\dot{s}_i^{vp}\} \tag{32}$$

where

$$
\left.
\begin{aligned}
&\{\dot{s}_i\} = \{\dot{s}_{\xi i},\ \dot{s}_{\theta i},\ \dot{s}_{\xi\theta i}\}^T \\
&\{\dot{s}_i^{vp}\} = \begin{Bmatrix} \dfrac{E_i}{E_0}\dfrac{\zeta}{a}\dfrac{1}{1-\nu_i^2}\dfrac{1}{C_1}\dot{m}_\xi^{vp} - \dot{s}_{\xi i}^{vp} \\ \dfrac{E_i}{E_0}\dfrac{\zeta}{a}\dfrac{1}{1-\nu_i^2}\dfrac{\nu}{C_1}\dot{m}_\xi^{vp} - \dot{s}_{\theta i}^{vp} \\ -\dot{s}_{\xi\theta i}^{vp} \end{Bmatrix} \\
&\zeta_{i-1} \leqq \zeta \leqq \zeta_i
\end{aligned}
\right\} \tag{33}
$$

$\{F_i\}$ and $\{H_i\}$ are determined from the shell geometries, the materials and the thickness of each layer.

By the use of Eqs. (17), (19) and (21), the rates of internal forces and stresses related to visco-plasticity are given as follows:

$$
\left.
\begin{aligned}
&\sigma_0 h_0 \sum_{n=0}^{\infty}\{\dot{n}_\xi^{vp(n)},\ \dot{n}_\theta^{vp(n)},\ \dot{n}_{\xi\theta}^{vp(n)}\}\quad [A_n] \\
&\quad = \sum_{i=1}^{n}\int_{\zeta_{i-1}}^{\zeta_i}\{\dot{\varepsilon}_\xi^{vp},\ \dot{\varepsilon}_\theta^{vp},\ \dot{\varepsilon}_{\xi\theta}^{vp}\}\quad [D_i]d\zeta \\
&(\sigma_0 h_0^3/a)\sum_{n=0}^{\infty}\{\dot{m}_\xi^{vp(n)},\ \dot{m}_\theta^{vp(n)},\ \dot{m}_{\xi\theta}^{vp(n)}\}\quad [A_n] \\
&\quad = \sum_{i=1}^{n}\int_{\zeta_{i-1}}^{\zeta_i}\{\dot{\varepsilon}_\xi^{vp},\ \dot{\varepsilon}_\theta^{vp},\ \dot{\varepsilon}_{\xi\theta}^{vp}\}\quad [D_i]\zeta d\zeta \\
&\sigma_0 \sum_{n=0}^{\infty}\{\dot{s}_\xi^{vp(n)},\ \dot{s}_\theta^{vp(n)},\ \dot{s}_{\xi\theta}^{vp(n)}\}\quad [A_n] \\
&\quad = \{\dot{\varepsilon}_\xi^{vp},\ \dot{\varepsilon}_\theta^{vp},\ \dot{\varepsilon}_{\xi\theta}^{vp}\}\quad [D_i]
\end{aligned}
\right\} \tag{34}
$$

The visco-plastic strain rates on the right-hand sides can be related to the stresses by Eq. (15).

3. Numerical Method

The incremental solutions at any calculation stage are obtained from Eqs. (29) with appropriate boundary conditions. Once these have been calculated, the increments of membrane forces and moments at any point in the shell can be found from Eqs. (25) and (26). The solutions at any time are given by summation of the incremental values. Equations (29) are solved numerically by the finite difference method as described in Ref. [5].

4. Numerical Example

As a numerical example of the multi-layered shells of revolution, a simply supported two-layered cylindrical shell composed of mild steel and titanium subjected to locally distributed loads is considered (Fig. 4).

The geometrical parameters of this shell are as follows:

$$
\left.
\begin{aligned}
&a=L,\ \xi=s/L,\ \rho=1/3,\ \omega_\theta=3 \\
&\rho'=\gamma=\omega_\xi=\omega'_\xi=0
\end{aligned}
\right\} \tag{35}
$$

The meridional mesh interval Δ in finite difference calculation is

$$\Delta = 1/2(N-1) \tag{36}$$

where N is the number of mesh points.

Boundary conditions at the points A and B are, respectively:

$$\dot{U}_\xi = \dot{U}'_\zeta = \dot{M}'_\xi = \hat{\dot{N}}_{\xi\theta} = 0 \tag{37}$$

and

$$\dot{U}_\theta = \dot{U}_\zeta = \dot{M}_\xi = \dot{N}_\xi = 0 \tag{38}$$

The material constants of mild steel and titanium employed in the calculations are as follows[14],[15],

Titanium:

$$
\left.
\begin{aligned}
&E = 9.1\times 10^4\ \text{MPa},\ \nu = 0.33 \\
&\gamma_1 = 8\,001/\text{s},\ \Phi(F) = \{(\bar{\sigma} - \sigma^*)/\sigma^*\}^{7.4} \\
&\sigma^* = 656(0.010\,1 + \bar{\varepsilon}^{vp})^{0.252}\ \text{MPa} \\
&\text{Initial yielding stress } \sigma_Y = 206.1\ \text{MPa}
\end{aligned}
\right\} \tag{39}
$$

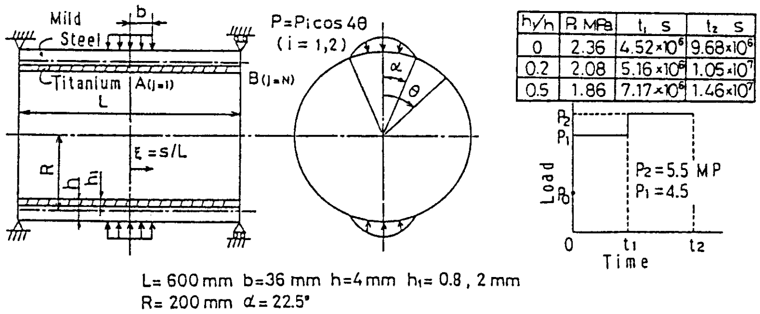

Fig. 4 Two layered cylindrical shell

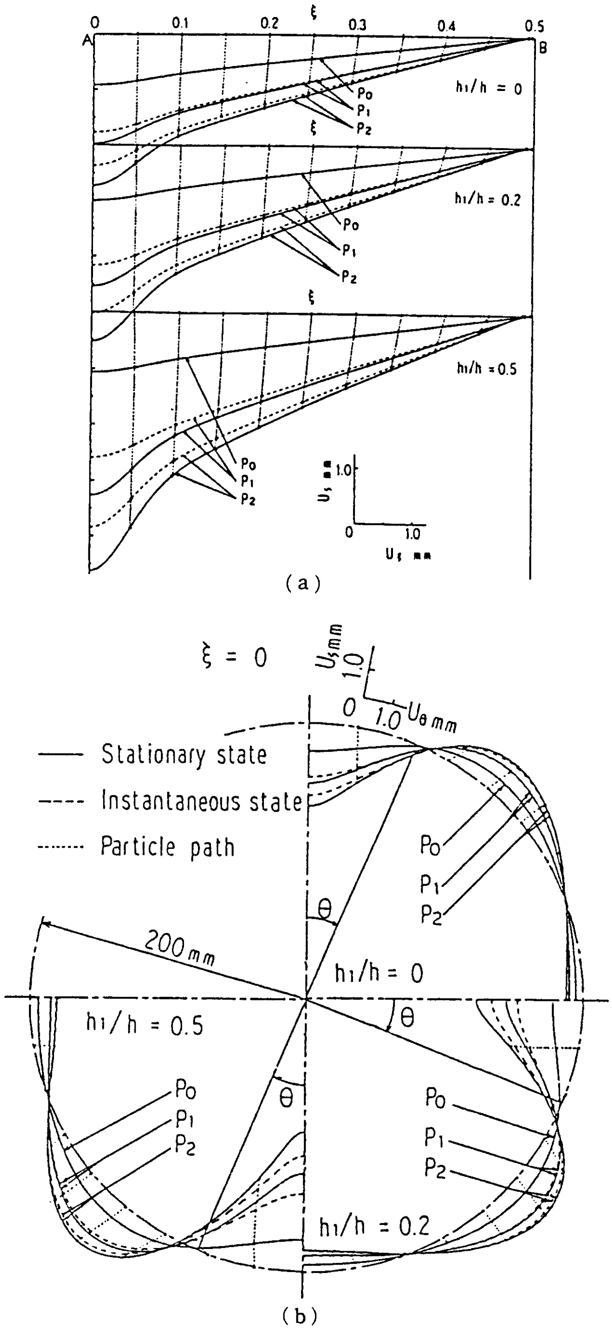

Fig. 5 Deformations

Mild steel:

$$\left.\begin{aligned}&E=2.0\times10^5\ \mathrm{MPa},\ \nu=0.29\\&\gamma_1=40.4\ 1/\mathrm{s},\ \Phi(F)=\{(\bar{\sigma}-\sigma^*)/\sigma^*\}^{5.0}\\&\sigma^*=261.7\ \mathrm{MPa}\end{aligned}\right\}\qquad(40)$$

The meridional mesh point number N and division number K through the thickness are selected as $N=51$ and $K=10$ for each layer. The number of terms of Fourier series is chosen to be 20. It is regarded that the stationary state has been reached when the ratio of maximum visco-plastic strain rate $\dot{\varepsilon}^{vp}_{max}$ to maximum strain ε_{max} immediately after each loading becomes less than 3.5×10^{-10}, i. e. $|\dot{\varepsilon}^{vp}_{max}/\varepsilon_{max}|\leqq3.5\times10^{-10}$.

These values are determined according to the convergency of the solution, the capacity of the computer and computing time.

Some of the essential features of the solutions are shown in Figs. 5-12. In the figures, the broken lines indicate the values immediately after loading of P_1 and P_2, and the solid lines indicate the values in stationary states. When $P=P_0$, initial yielding occurs on the outer surface at point A ($\xi=0$, $\theta=0$).

Figures 5(a) and (b) show the deformations of the cross section $\xi=0$ and those of meridional sections $\theta=0$ with time, respectively. The dotted lines indicate the particle path. The shell is greatly deformed at point A ($\xi=0$, $\theta=0°$). The difference between the instantaneous state and the stationary state incresses due to the progression of yielding with increasing loads. Shell deformations become large with the increased thickness of the titanium layer.

Figures 6 and 7 are the variations of distributions of N_ξ and N_θ with time. N_ξ relaxes more than N_θ in loading parts. The influence of h_1/h are not great.

Figures 8-10 show the meridional and circumferential distributions of the bending moments M_ξ and M_θ. They relax considerably with time in loading part. The variations become significant with increase of h_1/h, but there is little difference between the stationary values at each loading stage.

Figure 11 shows the yield progression. When $P=$

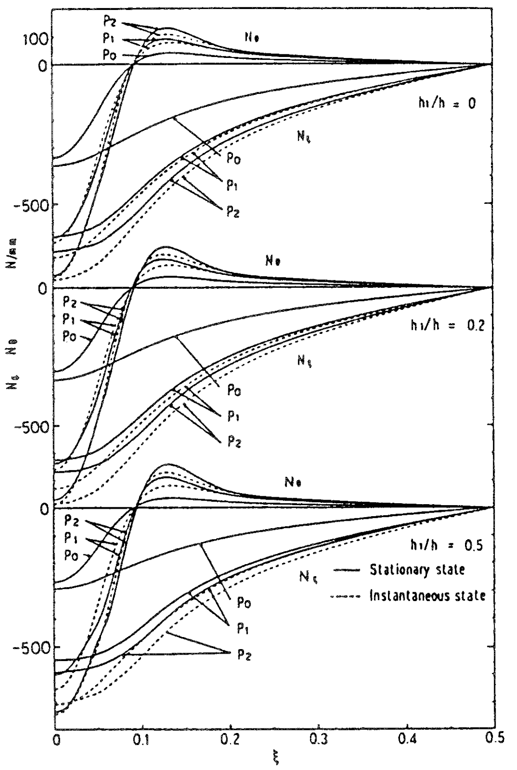

Fig. 6 Meridional distributions of N_ξ and N_θ

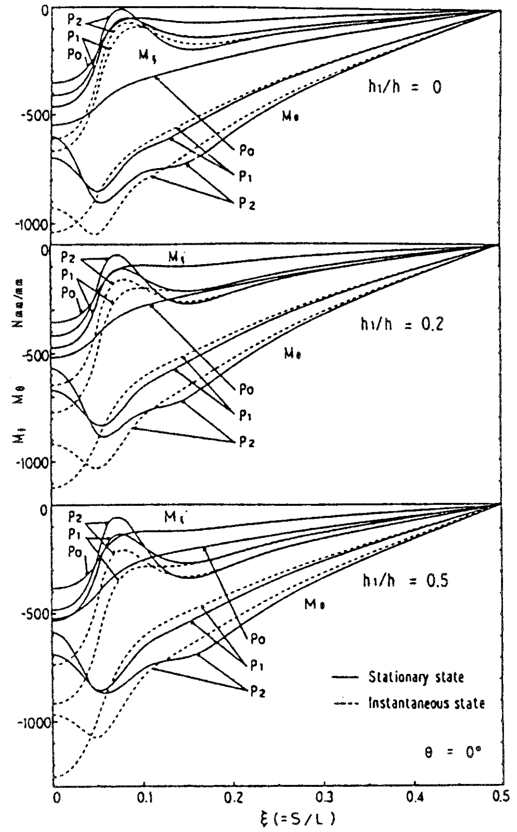

Fig. 8 Meridional distributions of M_ξ and M_θ

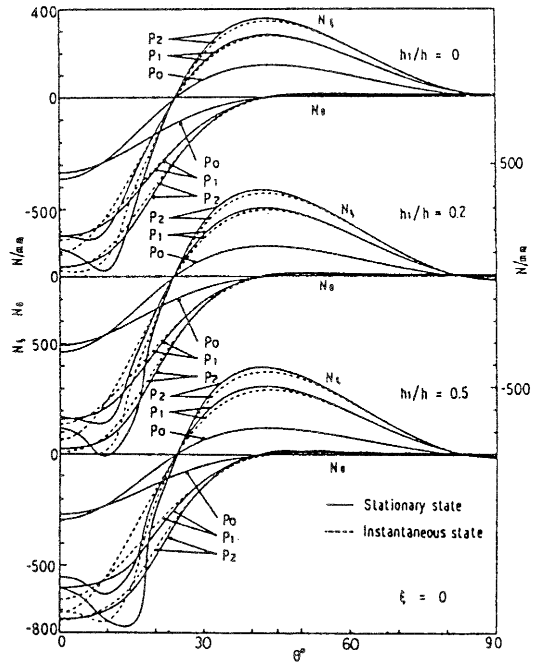

Fig. 7 Circumferential distributions of N_ξ and N_θ

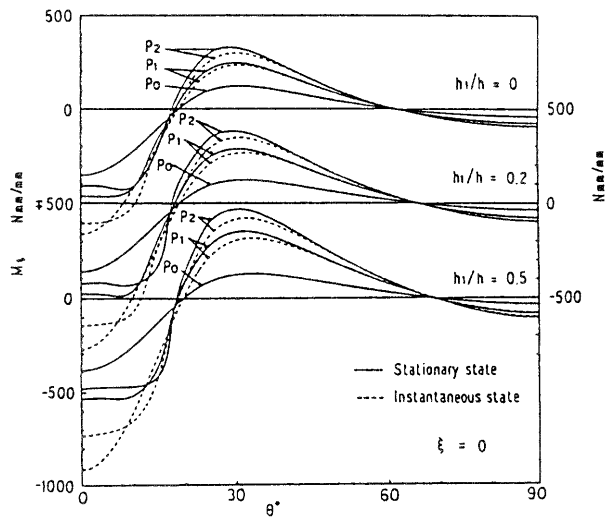

Fig. 9 Circumferential distributions of M_ξ

P_0, the initial yielding occurs on the outer-surface at point A. With the increase of loads P, the plastic zones progress from the loading part and the inner-surface at $\xi=0.09$ to the meridional and circumferential directions. The yielding zones of the two-layered shells are discontinuous on the interface and larger than those of the single-layered shell ($h_1/h=0$).

Figures 12 (a) and (b) show the distributions of stresses σ_ξ and σ_θ through the thickness at point A of the shell. The stresses relax in the outer part of the mild steel layer in every case of h_1/h. In the titanium layer, the stress variation is complex.

In numerical calculations, FACOM M-380 S+VP-100 was used. The CPU times of the numerical examples are about 20-40 minutes.

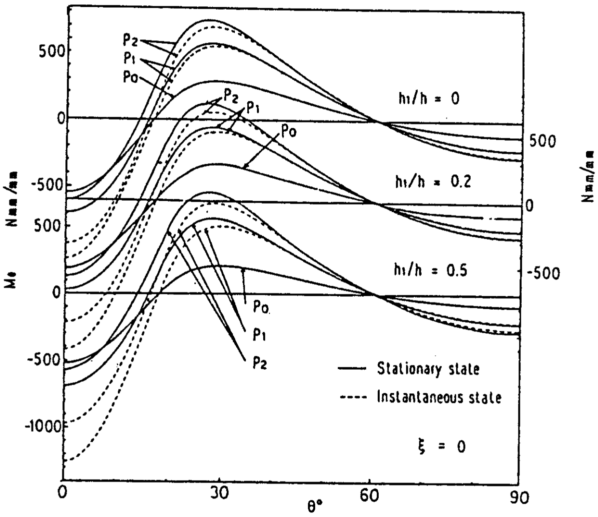

Fig. 10 Circumferential distributions of M_θ

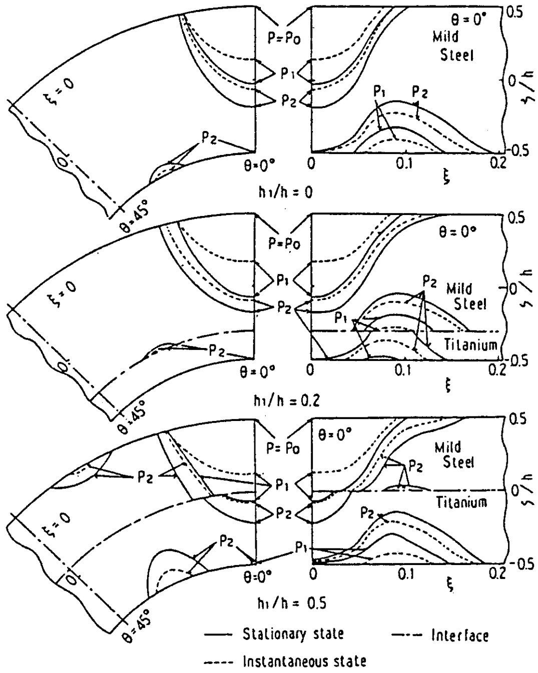

Fig. 11 Progression of yield

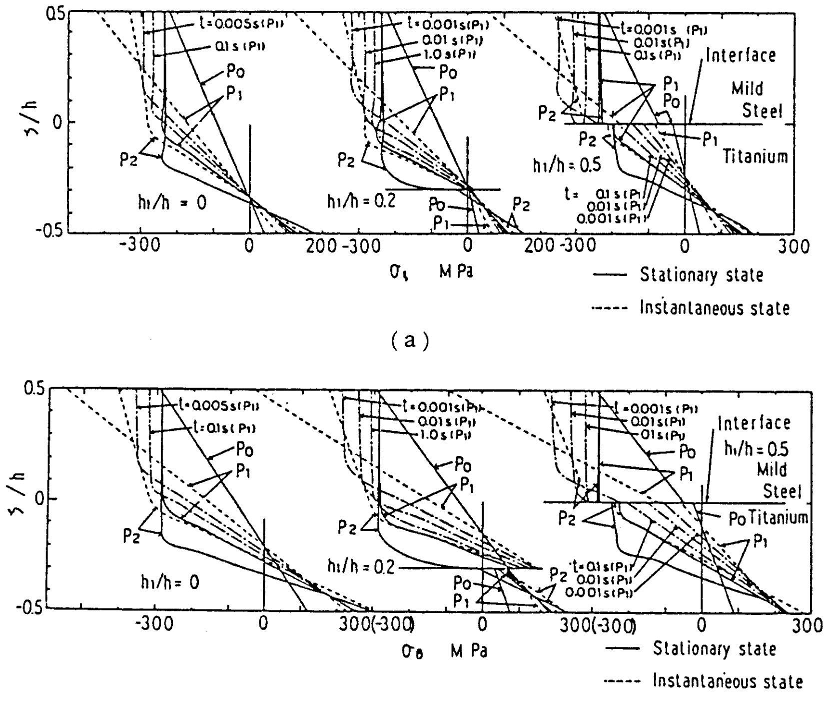

(b)

Fig. 12 Distributions of stresses through thickness of shell at point A ($\xi=0$, $\theta=0°$)

5. Conclusions

In this paper the authors have described the numerical analysis of elasto/visco-plastic problems of multi-layered shells of revolution under arbitrary loads. The basic differential equations on the multi-layered shell have been developed on the basis of Sanders' elastic shell theory. The elasto/visco-plastic equations by Perzyna have been employed as the constitutive relation.

The increments of all pertinent variables have been expanded into Fourier series in the circumferential direction and decoupled sets of ordinary differential equations have been solved by the usual finite difference method. The solutions at any time are obtained by integration of the incremental values.

As a numerical example of practical application, the creep deformation of a simply supported two-layered cylindrical shell composed of mild steel and titanium layers has been taken.

The numerical computations have been carried out for three cases of the ratio of thickness of titanium layer to shell thickness. It was found from the computations that the deformation becomes large with the increase of h_1/h and the stress distributions and progression of yield vary significantly depending on the thickness ratio.

References

(1) Zienkiewicz, O. C. and Owen, D. R. J., Analysis of Visco-Plastic Effects in Pressure Vessels by the Finite Element Method, Nucl. Eng. & Desn., Vol. 28 (1974), p. 278.

(2) Nagarajan, S. and Popov,E.P., Plastic and Visco-plastic Analysis of Axisymmetrical Shells, Intl. J. Solids and Struct., Vol. 11 (1975), p. 1.

(3) Takezono, S. and Tao, K., Elasto/Visco-Plastic Dynamic Response of Shells of Revolution, Trans. 4 th. Intl. Conf. on Struct. Mech. in Reactor Technol., Vol. M (1977-8), M 7/7.

(4) Takezono, S. and Akashi, T., Elasto/Visco-Plastic Deformations of Thin Shells of Revolution, Trans. 5th Intl. Conf. Struct. Mech. in Reactor Technol., Vol. M (1979), M 4/7.

(5) Tao, K. and Takezono, S., Elasto/Visco-Plastic Analysis of Axisymmetrical Shells under Asymmetrical Loading, Trans. 5th Intl. Conf. Struct. Mech. in Reactor Technol., Vol. M (1979), M 4/8.

(6) Takezono, S., Tao,K. and Kanezaki, K., Elasto/Visco-Plastic Dynamic Response of Axisymmetrical Shells by Overlay Model, ASME J. Pressure Vessel Technol., Vol. 102, No. 3 (1980), p. 257.

(7) Takezono, S. and Tao, K., Elasto/Visco-Plastic Dynamic Response of General Thin Shells to Blast Loads, Bull. JSME, Vol. 25, No. 203 (1982-5), p. 728.

(8) Atkatsh, R. S., Bieniek, M. P. and Sandler, I. S., Theory of Visco-plastic Shells for Dynamic Response, ASME J. Appl. Mech., Vol. 50, No. 1 (1983), p. 131.

(9) Kollmann, F. G. and Mukherjee, S., Inelastic Deformation of Thin Cylindrical Shells under Axisymmetric Loading, Ingenieur-Archiv Vol. 54 (1984), p. 355.

(10) Wojewodzki, W. and Bukowski, R., Influence of the Yield Function Nonlinearity and Temperature in Dynamic Buckling of Viscoplastic Cylindrical Shells, ASME J. Appl. Mech., Vol. 51, No. 2 (1984), p. 114.

(11) Takezono, S., Tao, K. and Nagano, S., Elasto/Visco-Plastic Analysis of Orthotropic Moderately Thick Shells of Revolution, Trans. 8th. Intl. Conf. on Struct. Mech. in Reactor Technol., Vol. L (1985), L 5/2.

(12) Takezono, S., Tao, K. and Uchibori, H., Elasto/Visco-Plastic Dynamic Response of Moderately Thick Shells of Revolution under Asymmetrical Loading. Proc. Intl. Conf. on Comput. Mech., Vol. 6 (1986), p. 41.

(13) Sanders, J. L., Jr., An Improved First-Approximation Theory for Thin Shells, NASA Technical Rep., R-24 (1959) p. 1.

(14) Perzyna, P., Fundamental Problems in Viscoplasticity, Advances in Appl. Mech., Vol. 9 (1966), p. 243, Academic Press.

(15) Takezono, S. and Satoh, M., Effect of Stress Frequency on Fatigue Crack Propagation in Titanium, ASME J. Eng. Mater. & Technol., Vol. 104, No. 4 (1982), p. 257.